Phase Transition and Doping induced Infrared Tunable Emission of $AgInS_2$ Luminescence Semiconductor

Yuan Chen,[1#] Gaoyuan Chen,[2,3#] Guijia Hu,[1,4] Hongcao Shi,[1] Xin Yang,[1,4] Ailijiang Abudurusuli,[5] Qi Sun,[5] Chunjian Su[1*]*

[1]*College of Mechanical and Electronic Engineering, Shandong University of Science and Technology, Qingdao, 266590, China.*

[2]*Key Laboratory of Intelligent Optoelectronic Devices and Chips of Jiangsu Higher Education Institutions, School of Physical Science and Technology, Suzhou University of Science and Technology, Suzhou, 215009, China.*

[3]*Advanced Technology Research Institute of Taihu Photon Center, School of Physical Science and Technology, Suzhou University of Science and Technology, Suzhou, 215009, China*

[4]*College of Energy Storage Technology, Shandong University of Science and Technology, Qingdao, 266590, China.*

[5]*MIIT Key Laboratory of Advanced Display Materials and Devices, College of Materials Science and Engineering, Nanjing University of Science and Technology, Nanjing 210094, China.*

[#]These authors contributed equally.

[*]Correspondence and requests for materials should be addressed to:

X.Y. (E-mail: *oyangx2003o@163.com*);

C.S. (E-mail: *suchunjian2008@163.com*).

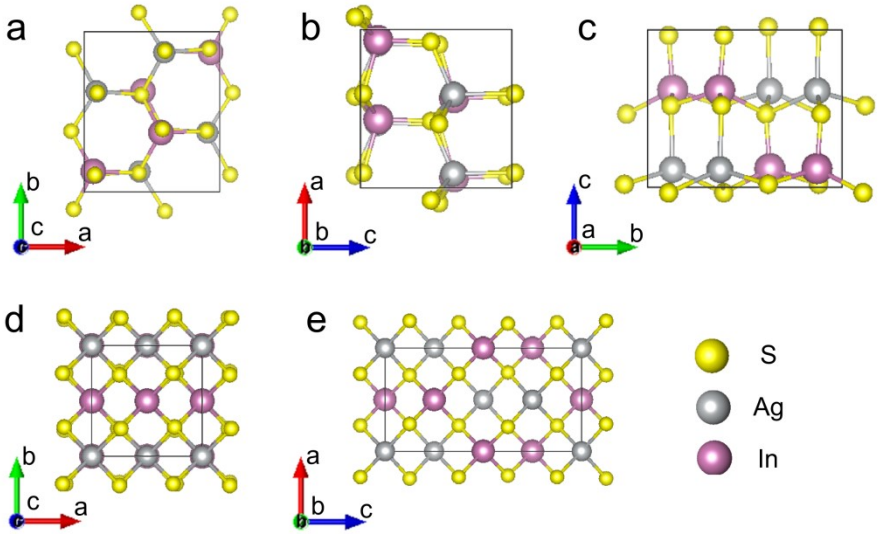

Figure S1. Schematic diagram of crystal structure for $AgInS_2$ orthorhombic (a-c), and tetragonal (d, e) along different directions view.

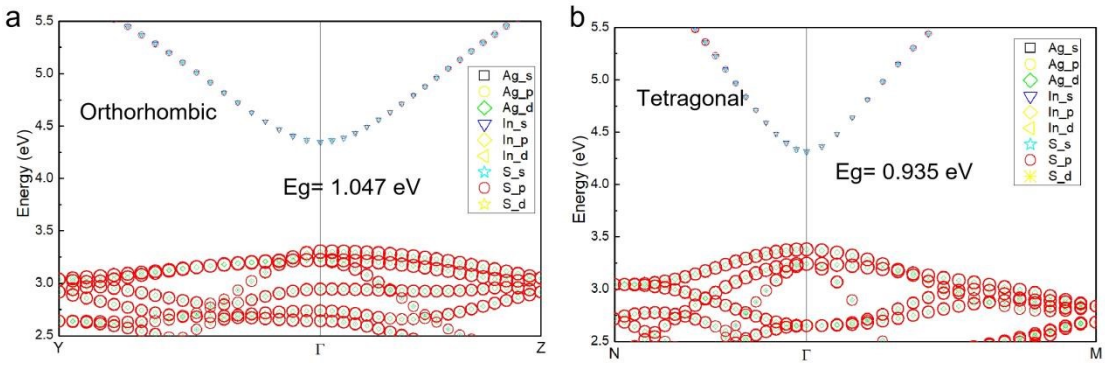

Figure S2. (a) XRD pattern of the $AgIn_5S_8$, the insert is the crystal structure. (b) PL spectra of the $AgIn_5S_8$ crystal. (DFT Calculated Electronic Band Structures and Density of States for AgInS2 Orthorhombic (a) and Tetragonal (b) Phases.)

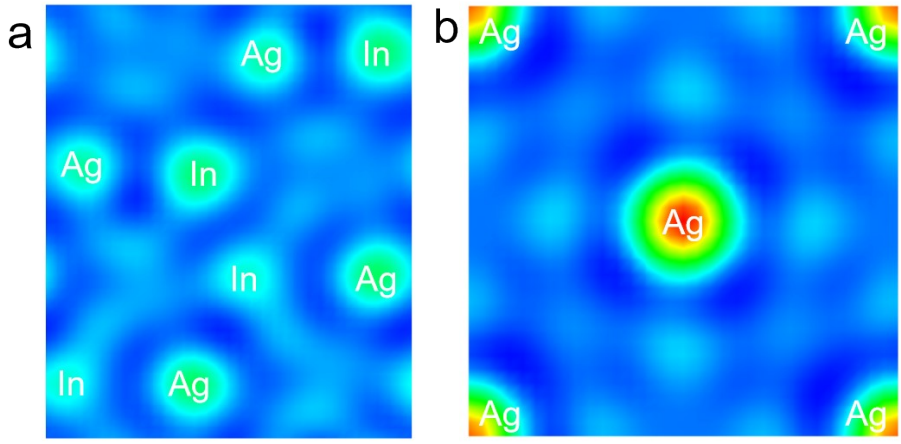

Figure S3. Charge density diagram of the $AgInS_2$ orthorhombic (a), and tetragonal (b).

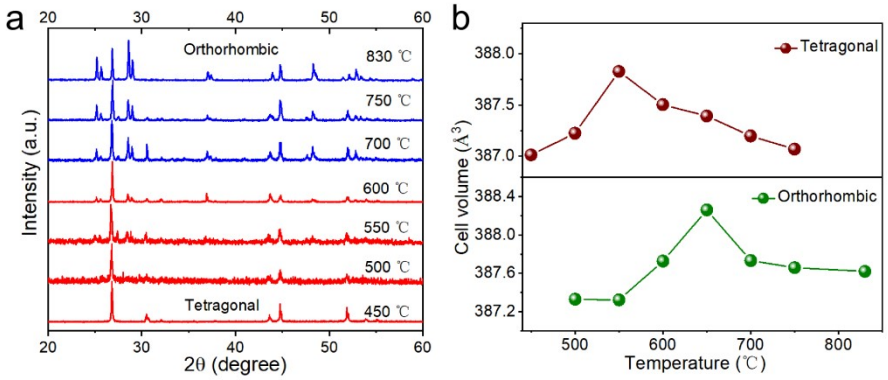

Figure S4. (a) XRD patterns of the $AgInS_2$ that produced from different temperature. (b) the cell volume revolution of the tetragonal and orthorhombic.

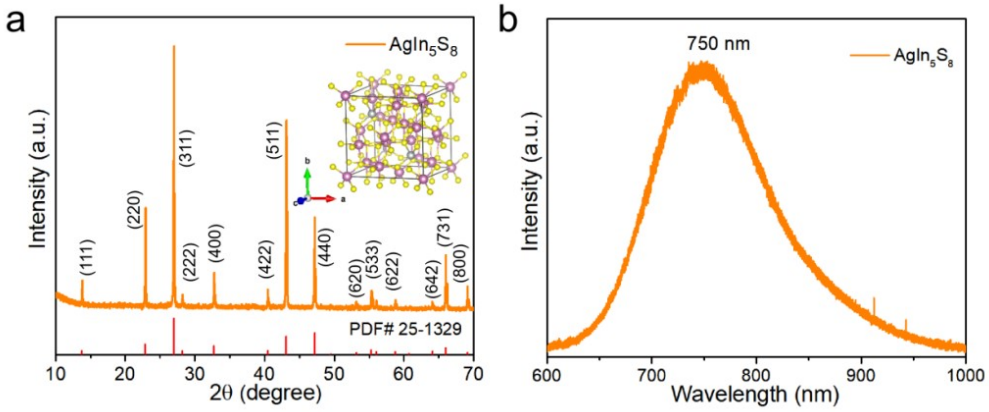

Figure S5. (a) XRD pattern of the $AgIn_5S_8$, the insert is the crystal structure. (b) PL spectra of the $AgIn_5S_8$ crystal.

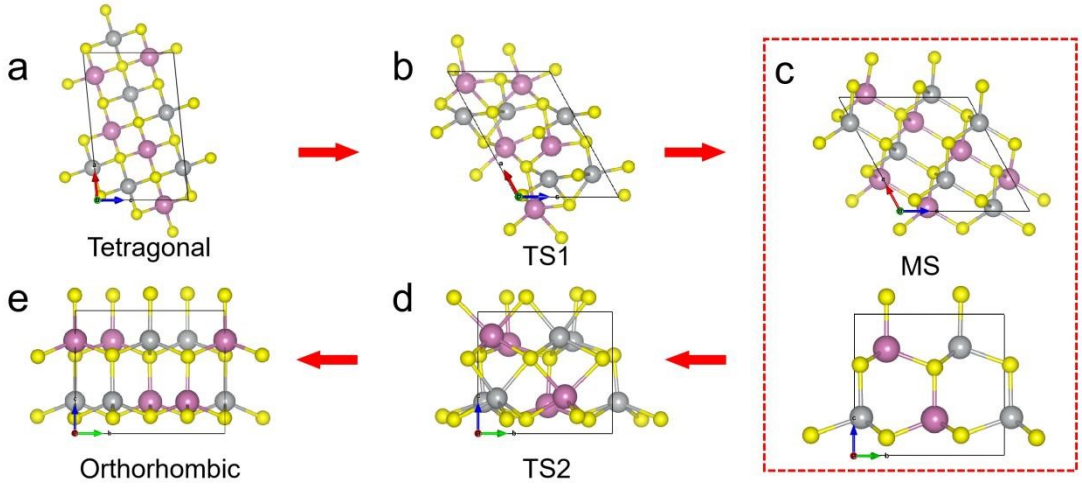

Figure S6. (a-e) Schematic diagram of the phase transition structure revolution from T→TS1→MS→TS2→O.

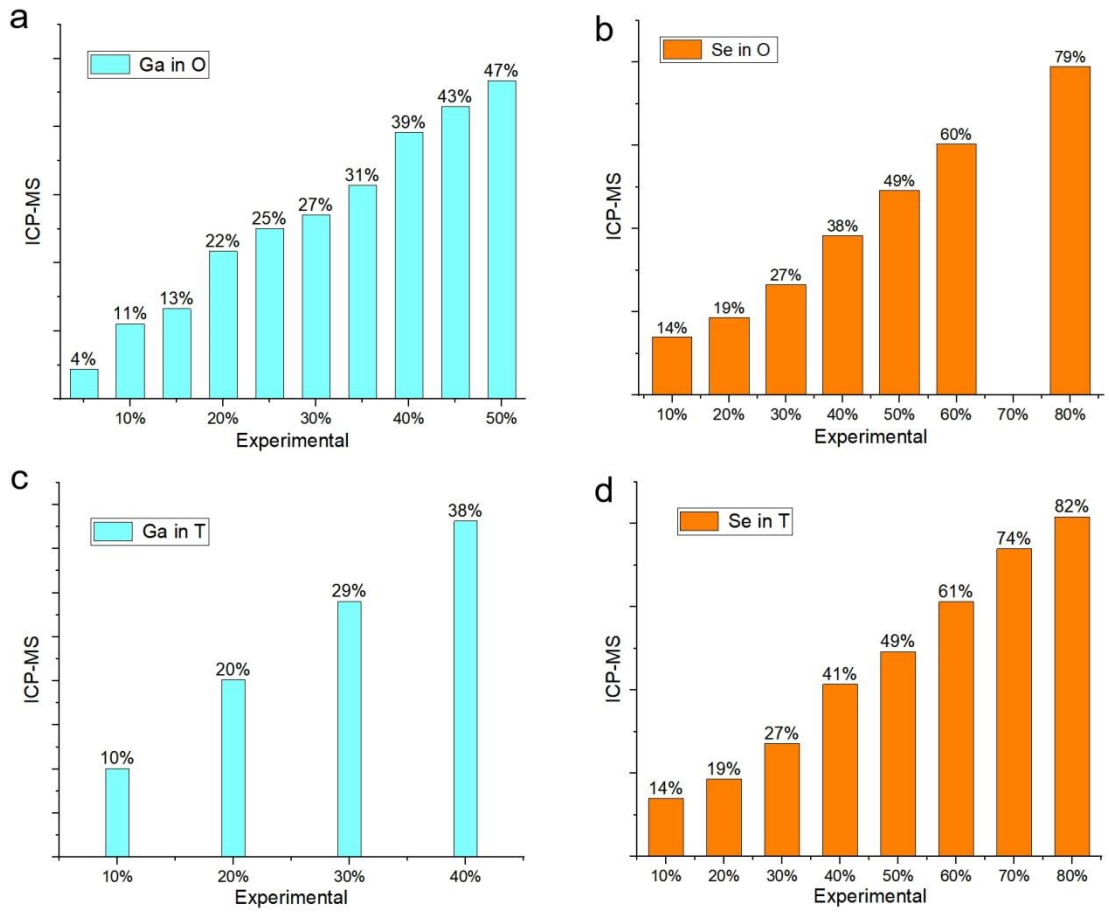

Figure S7. ICP-MS of the Se and Ga doping amount: (a) Se doping in O, (b) Ga doping in O, (c) Se doping in T, (d) Ga doping in T.

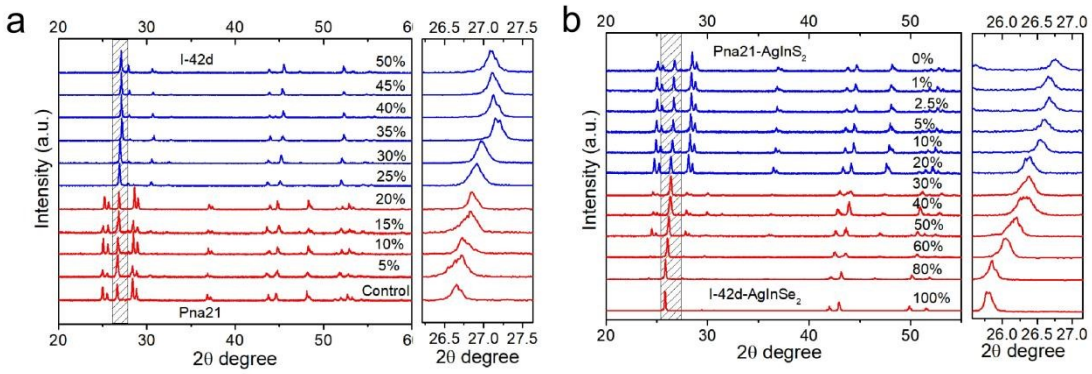

Figure S8. XRD pattern of the $AgInS_2$ doping with Ga (a) and Se (b), where, the orthorhombic is selected as host.

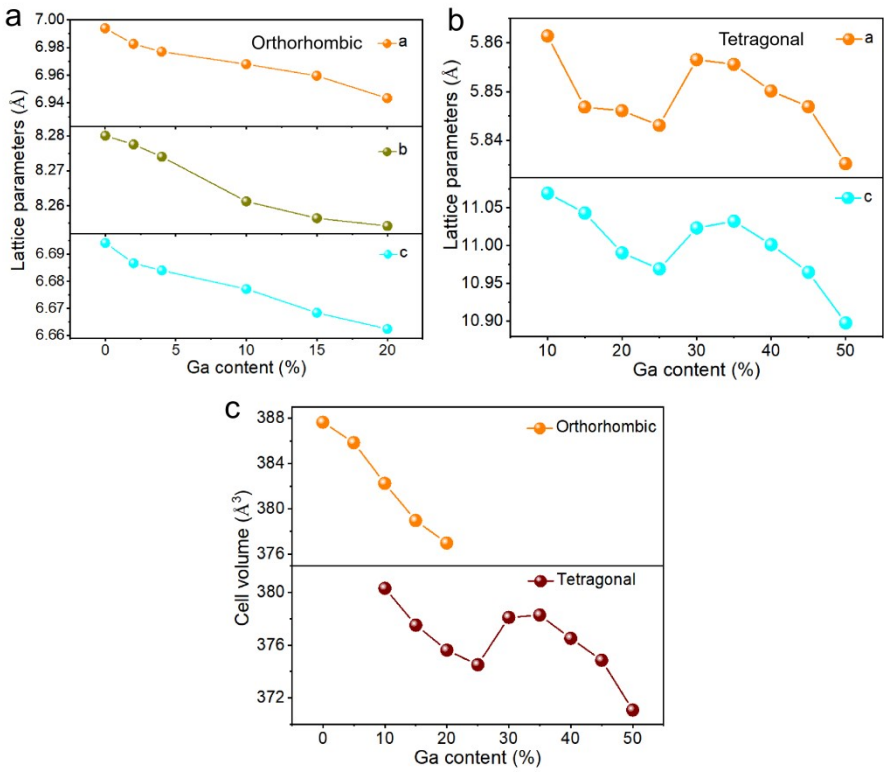

Figure S9.The lattice parameters (a, b) and cell volume (c) change as the Ga content increasing.

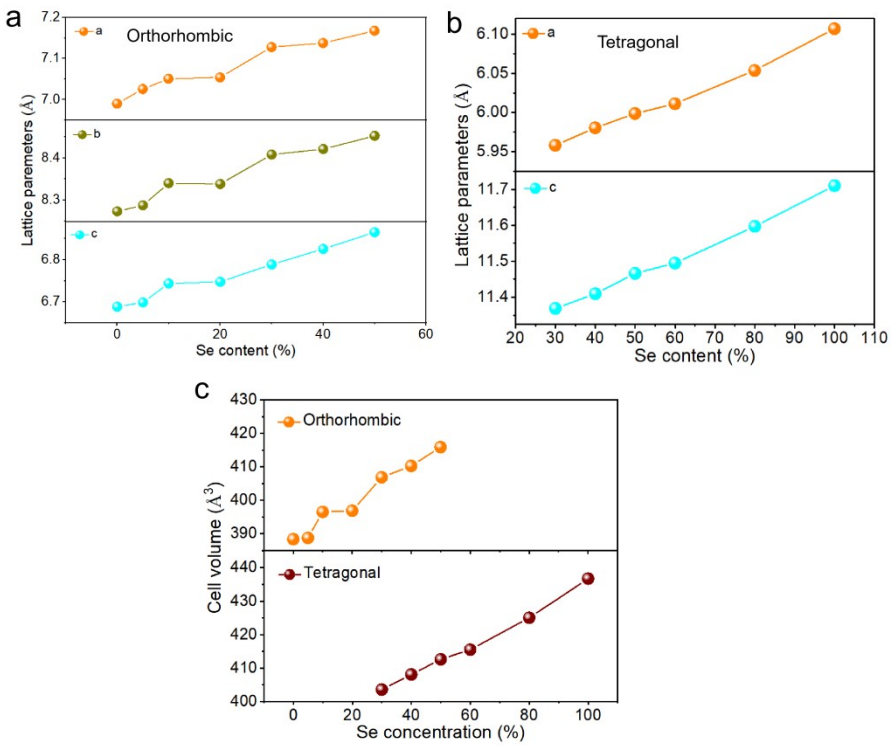

Figure S10. The lattice parameters (a, b) and cell volume (c) change as the Se content increasing.

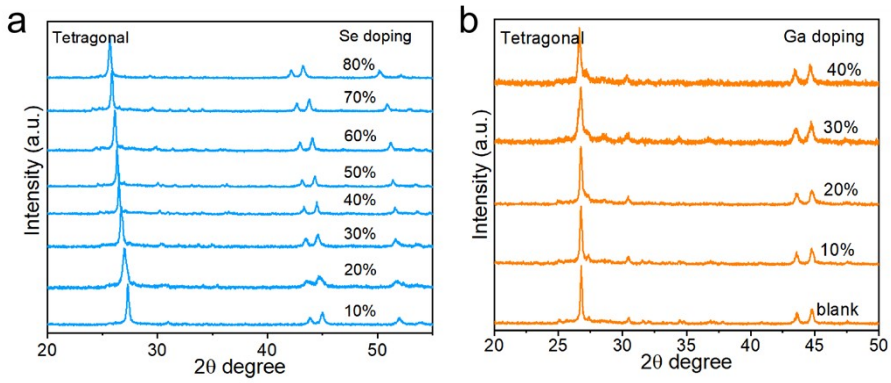

Figure S11. XRD pattern of the $AgInS_2$ doping with Ga (a) and Se (b), where, the host is tetragonal.

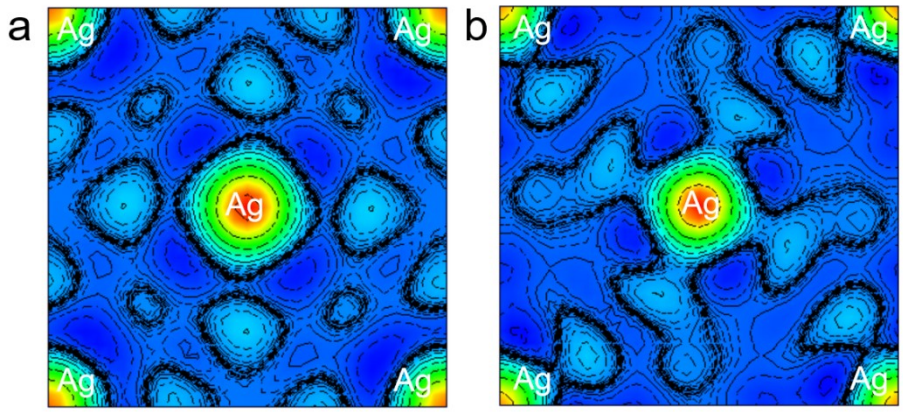

Figure S12. Charge density diagram of the $AgInS_2$ tetragonal (a) and Se 80% doping (b).

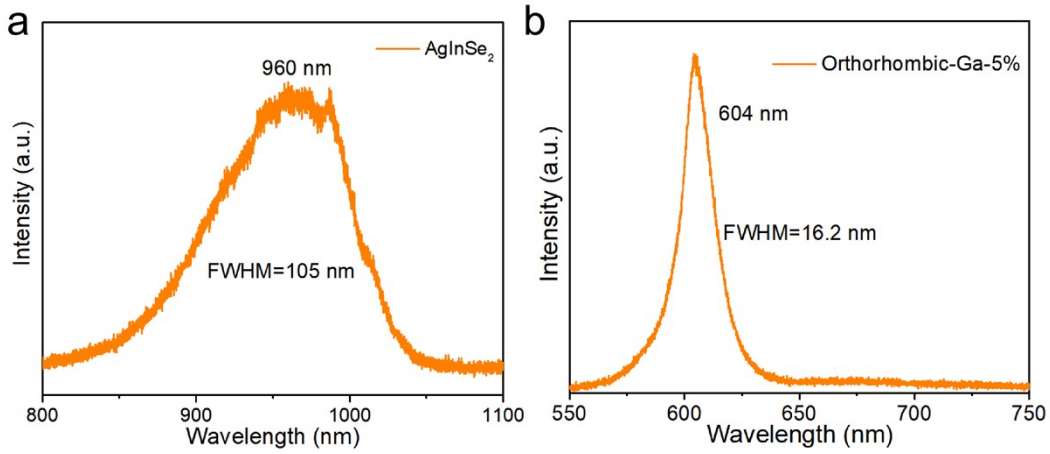

Figure S13. (a) PL pattern of the $AgInSe_2$ tetragonal. (b) PL pattern of the 5% Ga doped $AgInS_2$ orthorhombic.

Table S1. Crystallographic data for orthorhombic and tetragonal $AgInS_2$.

Empirical formula	$AgInS_2$	$AgInS_2$
Formula weight	286.69	286.69
Crystal system	Orthorhombic	Tetragonal
Space group	Pna21	I-42d
a (Å)	6.99006	5.8786
b (Å)	8.27351	5.8786
c (Å)	6.68837	11.2018
Volume ($Å^3$)	386.803	387.111
Density	4.926	4.921
χ^2	1.09	1.44
GOF	1.04	1.20
wR	12.156	14.7

Table S2. Structural data of $AgInS_2$ Orthorhombic phase

Crystal System	Orthorhombic	Space Group	Pna21	
Atom	Ag	In	S1	S2
Site Occupancy	1.00	1.00	1.00	1.00
x	0.40900	0.06700	0.09600	0.07800
y	0.12800	0.12900	0.62000	0.10800
z	0.11300	0.61800	0.01900	0.96500

Table S3. Structural data of $AgInS_2$ Tetragonal.

Crystal System	Tetragonal	Space Group	I-42d
Atom	Ag	In	S
Site Occupancy	1.00	1.00	1.00
x	0.00000	0.00000	0.26390
y	0.00000	0.00000	0.25000
z	0.00000	0.50000	0.12500

Table S4. Bond angle data for orthorhombic and tetragonal $AgInS_2$.

		[AgS4]	[InS4]
tetragonal	θ1	107.483	108.922
	θ2	113.526	110.575
orthorhombic	θ1	113.315	113.485
	θ2	110.169	110.282
	θ3	108.984	111.985
	θ4	103.706	103.628
	θ5	108.273	105.215
	θ6	112.275	111.892

Table S5. Calculated valance state of orthorhombic and tetragonal.

	tetragonal	orthorhombic
Ag	1.342	1.475
In	3.062	3.204
S1	-2.14	-2.316
S2	-	-2.362